

STUDYING THE POTENTIAL FOR MONITORING COLORADO RIVER ECOSYSTEM RESOURCES BELOW GLEN CANYON DAM USING LOW-ALTITUDE AVIRIS DATA

Erzsébet Merényi¹, William H. Farrand², Lawrence E. Stevens³, Theodore S. Melis⁴, Kapil Chhibber⁵

¹Lunar & Planetary Laboratory, University of Arizona, Tucson, AZ (erzsebet@lpl.arizona.edu)

²Space Science Institute, Boulder, CO (william.farrand@colorado.edu)

³Grand Canyon Wildlands Council, Flagstaff, AZ (farvana@aol.com)

⁴Grand Canyon Monitoring and Research Center, Flagstaff, AZ (tmelis@flagmail.wr.usgs.gov)

⁵University of Arizona, NASA Space Grant Program, Tucson, AZ (kapil@pirlmail.lpl.arizona.edu)

1. INTRODUCTION

Operational impacts of Glen Canyon Dam on downstream resources of the Colorado River ecosystem have been the subject of intense study and discussions among adaptive management stakeholders that include Federal, State and tribal entities, as well as recreational businesses, environmentalists, power companies, and others (U.S. Bureau of Reclamation 1995, Schmidt et al. 1998). The Grand Canyon Monitoring and Research Center (GCMRC within the U.S. Department of Interior) has identified the following key objectives for long-term monitoring of vital components of the ecosystem between Lakes Powell and Mead, while providing stakeholders with information for decision making: 1) lowest possible impact on critical resources; 2) highest possible return of integrated scientific information; and 3) long-term, repeatable data collection. Airborne hyperspectral image data are being considered as a possible long-term monitoring tool, which hold the promise of being able to fulfill the above requirements. The present study is a pilot project which is intended to explore the extent and variety of information, relevant for long-term monitoring, that can be extracted from images of both high spectral and spatial resolution.

The Colorado River ecosystem in Glen Canyon and Grand Canyon poses special challenges for remote monitoring with respect to logistics required to support field-based studies and relative to spatial scales at which monitoring is needed. The narrow corridor of the river is confined by tall vertical cliffs, yet provides a habitat for a great variety of both native and non-native plant species. Riparian vegetation consists of stands that often cover only very small areas. Often, these stands consist of intermixed native and non-native species, and spectral signatures of the various plants sometimes display only subtle differences. Adequate change detection mapping requires both high spectral and high spatial resolution, as well as advanced processing algorithms that can detect subtle spectral differences.

Change detection for evolving sand bars, rapids and debris fans is a critical part of the GCMRC's long-term monitoring program. Additionally, changes in the aquatic ecosystem's food base, such as abundance and distribution of algae and other benthic organisms are of great interest. Presently, the need to lower river stage for 2-3 days during annual monitoring overflights for conventional aerial photography and traditional surface measurements introduces artificial and undesirable impacts on the ecosystem (e.g., Blinn et al. 1999). With hyperspectral imagery, we expect to map riparian vegetation, terrestrial sediment deposits, as well as sand bars and benthic organisms through some depth of water, obtaining greater compositional information than can be obtained through the use of aerial photography.

1. AVIRIS DATA AND PREPROCESSING

Low altitude AVIRIS data were collected on October 4, 1998, in two runs. The data set comprises approximately 10 Gigabytes of data, divided into 10 image frames. These frames cover river miles -5.5 to -12.0, about 2.5% of the 300 miles long river corridor between Lake Powell and Lake Mead, and roughly 8% of the GIS study sites monitored by the GCMRC (Figure 1). The frame considered in this paper contains river miles -5.5 to -6.75, a portion of the river with a wide array of sediment and bedrock types and various typical aquatic and riparian

plant assemblages. The spatial resolution is approximately 2.7 m/pixel. North is shown at approximately ten – o’clock, and the river flows top to bottom in the frame. All four spectrometers functioned properly during the October 4 data acquisition. On 21 and 22 August 1998, field spectra of over 70 soil, rock and vegetation species were collected with an ASD FieldSpec FR, in areas that fall within our AVIRISLA image frames. A portion of these field spectra along with field photos of the respective species are posted at <http://www.lpl.arizona.edu/~erzsebet/index.html> , under “Ecosystem”.

GIS Monitoring Sites

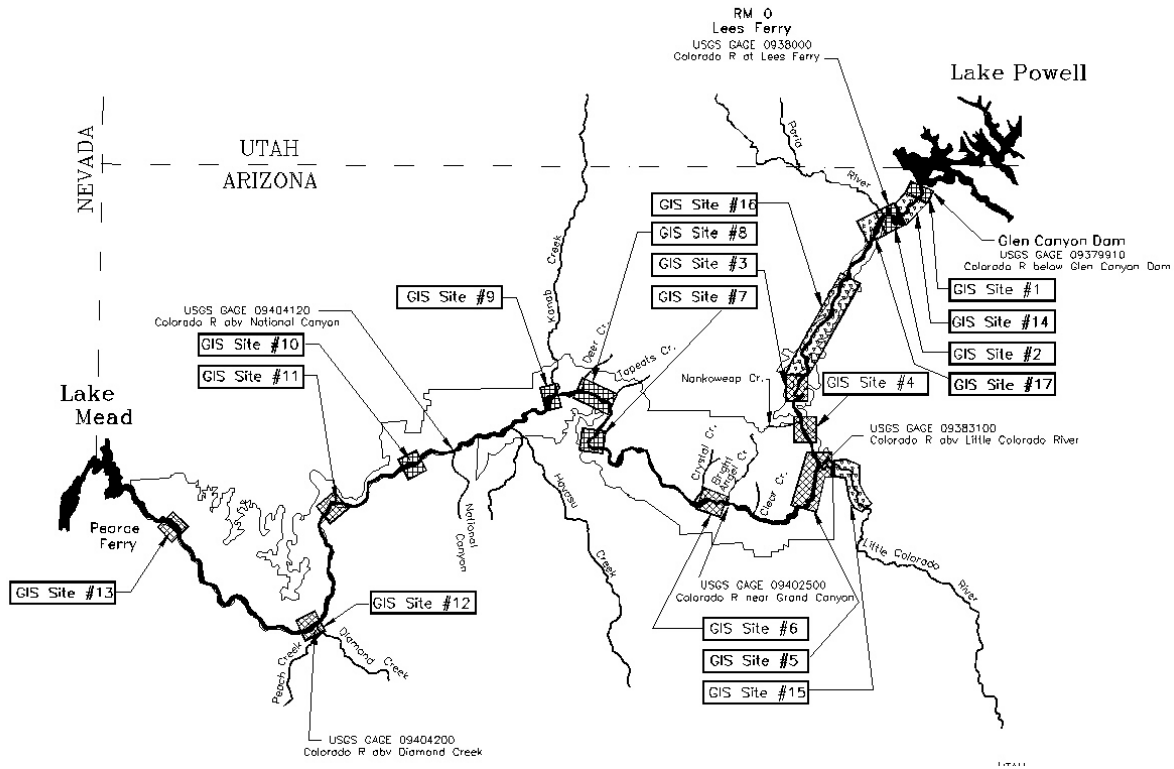


Figure 1. GIS monitoring sites of the Grand Canyon Monitoring and Research Center (GCMRC), along the Colorado River in Grand Canyon. The AVIRISLA imagery collected in October, 1998, coincides with GCMRC GIS Site #14. Figure courtesy of GCMRC.

The data received from the AVIRIS data lab had been geometrically rectified and registered (Boardman, 1999) and calibrated to at-sensor radiance. The image data in this study were then converted to apparent surface reflectance through the use of the ATREM program (Gao et al., 1993). In order to remove residual instrumental and atmospheric effects remaining after the ATREM correction, a second stage “modified flat field” (Farrand, 1992) correction was applied. This second stage correction consisted of the following steps: first, an average spectrum of three pixels covering a quartz sand bar that was visited during the August, 1998 field work was calculated. This average ATREM corrected spectrum was divided into each pixel in the ATREM corrected data cube. As part of the same mathematical operation, each pixel spectrum was multiplied through by a smoothed field spectrum of the sand bar. Further preprocessing included trimming off the no-data fringes, and elimination of the overlapping and excessively noisy bands, leaving 194 image bands. Before classification, a normalization (as described in Merényi et al., 1996) was also applied in order to cancel linear (i.e. terrain induced) shading effects. This treatment eliminates albedo differences; however, the benefits of normalization outweigh the disadvantages in most applications.

3. IMAGE ANALYSES AND RESULTS

Two independent analyses were performed: supervised classification by an Artificial Neural Net and Spectral Mixture Analysis. These are presented in Figures 2 and 3, respectively. The results were evaluated against field data that the GCMRC has accumulated over 20 years, against field spectra that were collected in August, 1998, and against the field knowledge of co-authors LS and TM. They have up-to-date, detailed knowledge of the spatial distribution of the resources mapped in this work, through their regular visits to the field (e.g., Stevens et al., 1995, 1997; Kaplinski et al., 1999).

3.1 Artificial Neural Network Classification

Supervised classification for 18 different surface covers was done using carefully selected training samples. The hybrid Artificial Neural Net (ANN) paradigm, which contains a Self-Organizing Map, is described in detail by Howell et al. (1994), Merényi et al. (1997), and Merényi (1998). For this task, 194 input neurons (corresponding to the number of spectral channels), a 40 x 40 hidden Self-Organizing layer, and 18 output neurons (one for each class) were applied. The software used is a collection of NeuralWare (1993) based classifiers and Khoros (Rasure and Young, 1992) based data exploration and other supporting tools, developed for hyperspectral imagery in-house at LPL, University of Arizona. The classes for which to train were determined on the basis of spectral variability found in the image. Identification of the spectral types (labeling the classes) was done by comparison to field spectra, and with the help of co-author LS. The resulting class map is shown in Figure 2. Mean spectra of classes are in Figure 4.

The greater surroundings of the river corridor in this section are dominated by red Navajo sandstone, which is mapped as class O and class N. Class O coincides with a nearly vertical cliff where dark MnO₂ coating (“desert varnish”) is common. Shading is also severe here due to the extreme geometry and it may cause as yet uninterpreted spectral effects. Class Q appears to be red sandstone where strong leaching of iron oxides has occurred. White alluvial and eolian sand (class P) is present in small sand beaches along the river. White sand is also exposed in the upper riparian zone (the “old high water line”, which was the 10 yr, pre-dam flood stage elevation), and it has been detected by this classification. The most obvious example is the nearly horizontal white linear feature toward the right side of the image, just above the bank at the inner curve of the river.

The water in this image has two significantly different segments. Class M shows no spectral signature of sediments. The water here is deep and obscures the sediments. Moreover, the very tall cliffs cast shadows, even at local noon when this image was taken, and further degrade the spectra. These effects will have to be investigated and calibrated. The river segment downstream of class M (downstream of the sharp diagonal dividing line at the cliff’s base near the center of the image) is less deep with no shadows cast on it. In this part, clear signatures of fine sediments (mainly sand) have been detected through the water. We attempted to map submerged sediments in three broad categories here: sediments under “shallow” water, under “deeper” water, and in the “deepest” part of the water. Class J represents sand banks under very shallow water. Training samples for this class were taken from the “L” shaped large sand bank close to the white sand beach just downstream of the dividing line of class M (Figure 2c). Note that a very small sand bank close to shore, under shallow water, was detected in the “deep water” section close to the top of the image (Figure 2b). Classes K and L map submerged sediments under two additional, progressively deepening water levels.

Algae-laden water, mapped as class I, corresponds well to known locations of shallow algal colonies, in distinct elongated patches along the shoreline.

Seven vegetation species were included in this classification. Redbud (*Cercis occidentalis*), a native tree, which grows in protected crevices up in the cliffs and away from the river (class F), and six riparian species. The latter are all represented on the sand beach in Figure 2b, which was one of the sites for our field work in August, 1998. Monitoring the spatial distribution of these species is an important concern as they make up the bulk of riparian habitat used by invertebrate and vertebrate fauna, and their distribution indicates or forecasts change in the ecosystem induced by variation in the flow regime or new (artificially introduced) components or by other factors (Stevens 1989). Tamarisk (*Tamarix ramosissima*), a widespread, non-native tree, is mapped as class A, and matches

the known, relatively large plant stands in this image frame. Arrow weed (*Tessaria sericea*, class B), partially decayed in the fall, and “Mixed grass” (primarily *Bromus* spp. and *Sporobolus* spp., class E) were recognized and mapped based on their field spectra, and generally correspond to ground truth, showing along shorelines. Training samples for coyote willow (*Salix exigua*, C), watersedge (*Carex aquatilis*, D), and seep willow (*Baccharis emoryi* and *B. salicifolia*, G) were identified from the site of our field work (Figure 2b) by our domain expert LS. The seep willow (G, maroon) on a sand bar, wedged diagonally into the large, 50-60 m wide, tamarisk stand and flanked by grass and coyote willows, is perfectly mapped. There are, however, some false indications of seep willow, showing as a linear feature at the border of the vegetation patch and the red rocks. This is due to the lack of additional training classes for “other leafy” vegetation that occurs there, and which may be spectrally very similar to the seep willow. The main coyote willow stand just above the white sand beach in Figure 2b is mapped faithfully, with a little overclassification to the left of the sand. The watersedge colony (D, dark green) along a backwater is also faithfully mapped, with the exception of a four pixel large (yellow) patch that was mis-classified as arrow weed. (The rest of the yellow feature is indeed arrow weed.)

One remaining vegetation class is a mixed one: grassy talus slope (H, orange), which shows at the right locations, from the border of vegetated patches up the slopes, more abundant in drainages than elsewhere. This class exhibits both rock and grass signature. In addition, an “unknown” material was noticed (R, lilac), which is as yet unidentified. Several, spatially coherent, unclassified areas indicate that the classification can be refined to include more classes. Examples of this are the unclassified ring around the large L-shaped submerged sand bar (class J), which is probably lined with cobbles at the bottom; or the large unclassified spot on the outer bank at the bend of the river, which may be a plant or rock type, different enough spectrally that it was not assigned to any of the present classes.

3.2 Endmember Determination and Mapping

One of the processing approaches used on the AVIRIS scene considered here was an approach using processing tools resident in the ENVI software package (RSI, 1997). The data were transformed using a Minimum Noise Fraction (MNF) transform. A small number of endmembers were determined by examining two dimensional scatterplots in which the first several MNF bands were successively plotted against each other and pixels at the vertices of the observed data clouds were selected. Using averages of these pixels, the data were reduced via Spectral Mixture Analysis (SMA) (Adams et al., 1993). A good set of fraction images with a relatively bland RMS error image was derived using just three endmembers: a “white” (relatively ferric oxide free) rock, a “red” (ferric oxide – rich) rock, and green vegetation. From the RMS error image, a number of spatially restricted materials were identified including white sand beaches and submerged sediments. A region of interest (ROI) was defined by thresholding the vegetation fraction image. The first six MNF bands were interactively examined using the ENVI n-dimensional visualization tool using the vegetation-rich pixels as the input ROI. In this way, a number of distinct vegetation classes were identified. Several of the more spectrally distinct vegetation classes along with the two rock endmembers and the “submerged sediments” and “white sand” materials (identified in the SMA RMS error image) were used as the target materials for a Spectral Angle Mapper (SAM) classification which is presented here as Figure 3.

The eight species mapped by SAM classification include three terrestrial vegetation types, three rock/soil types and two “in-water” species. Classes 1, 2 and 3 mostly match the coyote willow, arrow weed, and tamarisk, respectively, in the ANN classification (Figure 2). Classes 5, 6, and 7 are the same as classes O, N, and P in Figure 2. Class 3 appears to coincide with class R of the ANN map, and class 8 does not match any of the ANN classes.

4. SUMMARY AND FUTURE IMPROVEMENTS

The remote sensing and analysis approaches used here show great promise for ecosystem monitoring in Grand Canyon, and elsewhere. Further refinement of these techniques using existing imagery will provide a basis for expanding the scope of coverage to other GIS reaches, which are presently being monitored through costly, intrusive, on-the-ground approaches. These techniques offer important new analytical tools for evaluating and monitoring other ecosystems, on earth and elsewhere.

We mapped eight vegetation species, 5 “in-water” species such as algae plus submerged sediments, and four rock/soil types from a low-altitude AVIRIS image covering the –5.5 to –6.75 river miles of the Colorado River

in Glen Canyon. The 2.7 m/px spatial resolution allowed very detailed mapping of plant stands that are important to distinguish and monitor, on the few meters scale. The presented analyses are in good agreement with ground truth.

In this first attempt we achieved a goal of mapping underwater sediments, with a qualitative distinction among three levels of water covering the sediments. As resources allow, future work will include more gradations, and more quantitative assessment of water depth and distinguishing among sand, cobbles and other materials underwater.

More vegetation species can be readily included in future classifications. For example, the pixels misclassified for seep willow (G, maroon class) will be examined and made into one or more appropriate new classes. Similarly, the unclassified terrestrial patches will be evaluated and included as a refinement to the present classification. Then, the area coverage of each class will be calculated by multiplying the number of pixels in the class by 2.7 x 2.7 square meters.

We plan to analyze three more AVIRISLA frames of the Glen Canyon reach, that will extend the mapping discussed here up to river mile -9. With that we will have a significant statistical basis for the evaluation of the powers of high spatial resolution hyperspectral imaging as a potential monitoring approach. In addition, resources permitting, imagery in a downstream reach (river mile +7.9) will be evaluated for terrestrial features with coarse sediment textures, such as debris fans and rapids.

5. ACKNOWLEDGEMENTS

EM is funded for development of neural net tools by NASA, OSSA Applied Information Systems Research Program, NAG54001. KCh is supported by NASA's Space Grant Program. The Grand Canyon Monitoring and Research Center provided all support for the August, 1998 field work, and we thank M. Liszewski and his staff for field assistance. Further field studies by LS and EM were part of a research raft trip, supported by GCMRC and the National Park Service. The ASD FieldSpec FR instrument and expertise were graciously provided by the Remote Sensing Group of the University of Arizona. The authors are grateful to the JPL AVIRIS team for collecting and making available the geometrically reconstructed low-altitude AVIRIS imagery.

6. REFERENCES

Adams, J.B., M.O. Smith, and A.R. Gillespie, 1993, "Imaging spectroscopy: Interpretation based on spectral mixture analysis", in *Remote Geochemical Analysis: Elemental and Mineralogical Composition*, edited by C.M. Pieters and P.A.J. Englert (New York: Cambridge University Press), pp. 145-166.

Blinn, D.W., J.P. Shannon, K.P. Wilson, C.O'Brien, and P.L. Benenati, 1999, "Response of benthos and organic drift to a controlled flood", in *The controlled flood in Grand Canyon* edited by R.H. Webb, J.C. Schmidt, G.R. Marzolf, and R.A. Valdez. American Geophysical Union Geophysical Monograph 110, pp. 259-272.

Boardman, J.W., 1999, "Precision Geocoding of Low-Altitude AVIRIS Data: Lessons Learned in 1998", *Summaries of the Eighth Airborne Earth Science Workshop, AVIRIS Workshop*.

Farrand, W.H., 1992, "A comparison of methods for retrieving apparent surface reflectance from hyperspectral data", *Proc. of the International Symposium on Spectral Sensing Research*, 1154-1164.

Gao, B.C., K.B. Heidebrecht, and A.F.H. Goetz, 1993, "Derivation of scaled surface reflectances from AVIRIS data", *Remote Sens. Environ.*, vol. 44, no. 2/3, pp. 165-178. Howell, E.S., E. Merenyi, and L.A. Lebofsky, 1994, "Classification of asteroid spectra using a neural network", *Journal Geophys. Res.*, vol 99, pp 10,847-10865.

Kaplinski, M.K., J.E. Hazel, R. Parnell, and M. Manone, 1999, "Monitoring fine-sediment storage of the Colorado River ecosystem below Glen Canyon Dam, Arizona", *Annual Fact Sheet of the Northern Arizona University Geology Department, Flagstaff, AZ*, 4 p.

- Merényi, E., Singer, R.B., and Miller, J.S., 1996, "Mapping of Spectral Variations on the Surface of Mars from High Spectral Resolution Telescopic Images", *Icarus*, vol. 124, pp. 280–295.
- Merényi, E., E.S. Howell, A.S. Rivkin, and L.A. Lebofsky, 1997, "Prediction of Water in Asteroids from Spectral Data Shortward of 3 microns", *Icarus*, vol 129, pp 421-439.
- Merényi, E., 1998, "Self-Organizing Maps for Planetary Surface Composition Research", Proc. European Symposium on Artificial Neural Networks, Bruges, Belgium, April 22-24, 1998, pp. 197-202. [Downloadable from <http://www.lpl.arizona.edu/~erzsebet/emann.html>]
- NeuralWare, Inc., 1993, "Neural Computing", *NeuralWorks Professional II/Plus, Neural Computing*, NC:293-305.
- Rasure , J., and M. Young, 1992, "An Open Environment for Image Processing Software Development, *Proc. Of the SPIE/IS&T Symposium in Electronic Imaging, February 14, 1992*, vol. 1659.
- Research Systems Inc., 1997, *ENVI v.3 User's Guide*, RSI, Boulder, 614 pp.
- Schmidt, J.C., R.H. Webb, R.A. Valdez, G.R. Marzolf, and L.E. Stevens, 1998, "Science and values in river restoration in the Grand Canyon", *Bioscience* vol 48, pp. 735-747.
- Stevens, L.E., 1989, "Mechanisms of riparian plant community organization and succession in the Grand Canyon, Arizona", Northern Arizona University PhD Dissertation, Flagstaff.
- Stevens, L.E., J.C. Schmidt, T.J. Ayers, and B.T. Brown, 1995, "Flow regulation, geomorphology, and Colorado River marsh development in the Grand Canyon", *Ecological Applications* vol 5, pp. 1025-1039.
- Stevens, L.E. J.P. Shannon and D.W. Blinn, 1997, "Benthic ecology of the Colorado River in Grand Canyon: dam and geomorphic influences", *Regulated Rivers: Research & Management* vol 13, pp. 129-149.
- U. S. Department of Interior, Bureau of Reclamation. 1995, "Operation of Glen Canyon Dam, Colorado River Storage Project, Arizona, Final Environmental Impact Statement", U.S. Govt. Printing Office 1995-841:509, Washington, DC.

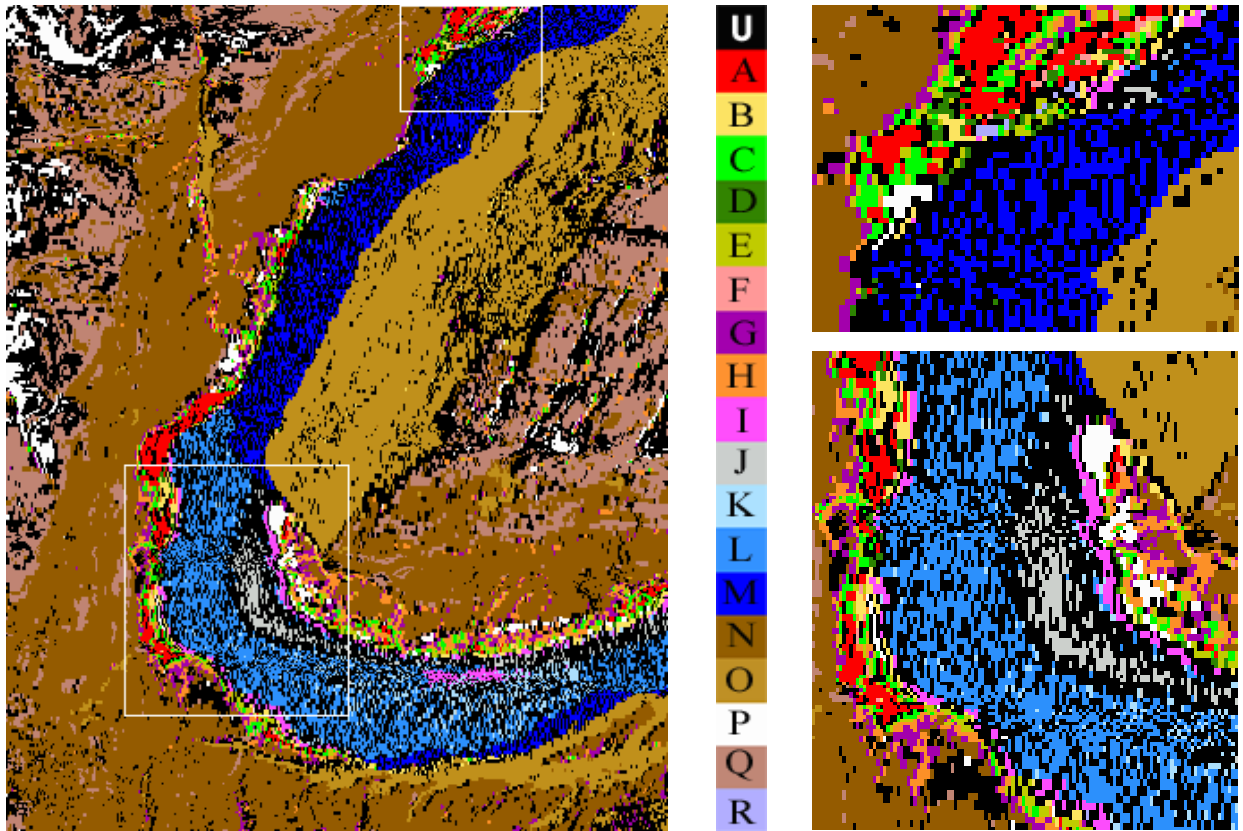


Figure 2. (upper half of page) **a) Left:** Artificial Neural Network classification. U – Unclassified ; A – Tamarisk; B – Arrow weed, partially decayed; C – Coyote willow; D – Watersedge; E – Mixed grass, green and dry; F – redbud tree; G – Seep willow on sand ridge; H – Grassy talus slope; I – Algae-laden water; J – Submerged sediments 1; K – Submerged sediments 2; L – Submerged sediments 3; M – Deep water and/or very dark shadow, no sediments seen; N – Red sand; O – Red Navaho sandstone; P – White sand; Q – Bluff colored Navajo sandstone; R – Unknown; **b) Top right:** Enlargement of the upper boxed area in a). **c) Bottom right:** Enlargement of the lower boxed area in a).

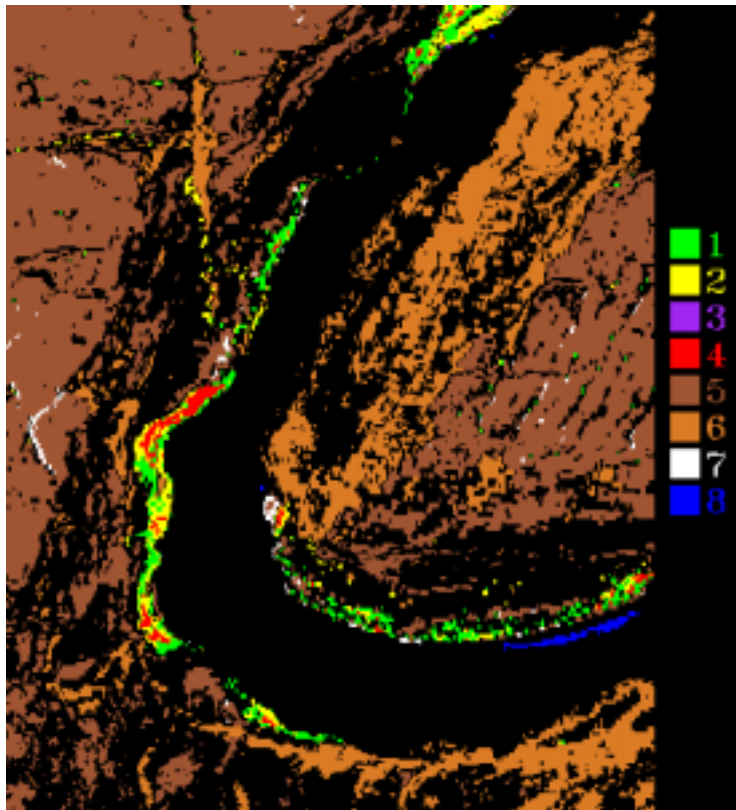


Figure 3. (left) Spectral Angle Mapper classification of endmembers determined from Spectral Mixture Analysis. 1 – vegetation 1; 2 – vegetation 2; 3 – in-water vegetation; 4 – vegetation 3; 5 – bluff colored Navajo sandstone; 6 – red colored Navajo sandstone; 7 – white sand beach; 8 – submerged sediments.

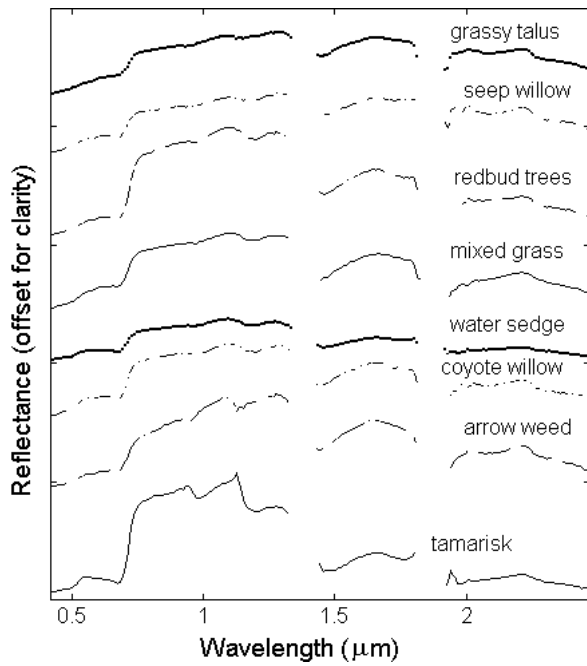
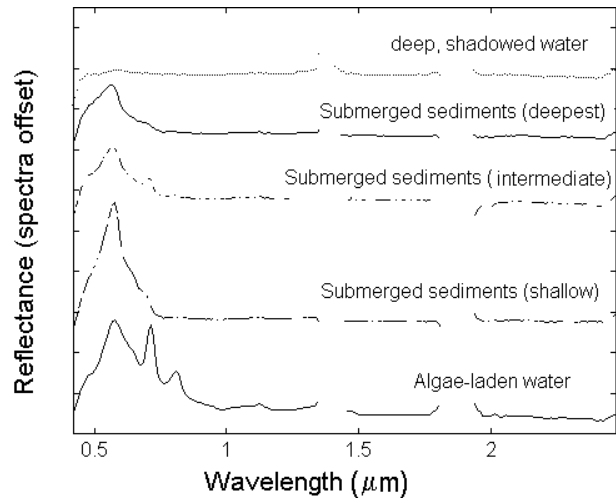
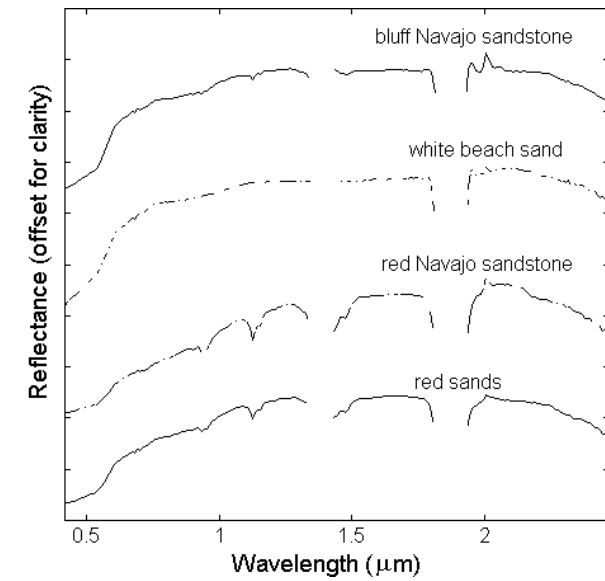


Figure 4. Representative spectra of the species mapped by Artificial Neural Net classification in Figure 2.

a) (upper left) Spectra of rocks and soils; **b)** (upper right) Spectra of “in-water” species; **c)** (left) Spectra of vegetation species.